JACS
JOURNAL OF THE AMERICAN CHEMICAL SOCIETY
Article
pubs.acs.org/JACS

Biosynthetic Pathway for the Epipolythiodioxopiperazine Acetylaranotin in *Aspergillus terreus* Revealed by Genome-Based Deletion Analysis

Chun-Jun Guo,[†] Hsu-Hua Yeh,[†] Yi-Ming Chiang,[†,§] James F. Sanchez,[†] Shu-Ling Chang,[†,∥] Kenneth S. Bruno,[‡] and Clay C. C. Wang*[,†,⊥]

[†]Department of Pharmacology and Pharmaceutical Sciences, School of Pharmacy, University of Southern California, Los Angeles, California 90089, United States

[‡]Chemical and Biological Process Development Group, Energy and Environment Directorate, Pacific Northwest National Laboratory, Richland, Washington 99352, United States

[§]Graduate Institute of Pharmaceutical Science, Chia Nan University of Pharmacy and Science, Tainan 71710, Taiwan

[∥]Department of Biotechnology, Chia Nan University of Pharmacy and Science, Tainan 71710, Taiwan

[⊥]Department of Chemistry, College of Letters, Arts, and Sciences, University of Southern California, Los Angeles, California 90089, United States

Supporting Information

ABSTRACT: Epipolythiodioxopiperazines (ETPs) are a class of fungal secondary metabolites derived from diketopiperazines. Acetylaranotin belongs to one structural subgroup of ETPs characterized by the presence of a seven-membered 4,5-dihydrooxepine ring. Defining the genes involved in acetylaranotin biosynthesis should provide a means to increase the production of these compounds and facilitate the engineering of second-generation molecules. The filamentous fungus *Aspergillus terreus* produces acetylaranotin and related natural products. Using targeted gene deletions, we have identified a cluster of nine genes (including one nonribosomal peptide synthetase gene, *ataP*) that is required for acetylaranotin biosynthesis. Chemical analysis of the wild-type and mutant strains enabled us to isolate 17 natural products from the acetylaranotin biosynthesis pathway. Nine of the compounds identified in this study are natural products that have not been reported previously. Our data have allowed us to propose a biosynthetic pathway for acetylaranotin and related natural products.

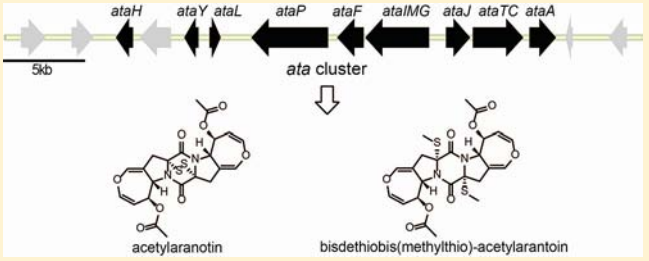

INTRODUCTION

Epipolythiodioxopiperazines (ETPs) are a class of secondary metabolite toxins originating from diketopiperazines (DKPs).[1] One distinct feature of ETPs is the presence of unique di- or polysulfide bridges. This rare structural motif is hypothesized to mediate molecular toxicity in at least two ways: (1) by cross-linking vital proteins via cysteine bonds or (2) by redox cycling to form reactive oxygen species (ROS), which can cause severe damage to the host cells.[1] The taxonomic distribution of ETPs among fungi is discontinuous, but at least 14 ETPs have been characterized from a diverse range of filamentous fungi.[1,2] The best-characterized ETP, gliotoxin (Figure 1), was identified in the opportunistic pathogen *Aspergillus fumigatus*. A recent study has shown that gliotoxin induces apoptosis in mammalian cells by activating the proapoptotic Bcl-2 family member Bak.[3] Activation of the Bak protein elicits the generation of ROS and the release of apoptogenic factors by the mitochondria.[3] Gliotoxin has also been found to be an inhibitor of the transcription factor NF-κB.[4] Since this factor plays an integral role in the inflammatory immune response, the inhibitory effect of gliotoxin may account for the immunosuppressive properties of some ETPs.[4] Another ETP, acetylaranotin (**1**) (Figure 1), was first isolated from *Arachniotus aureus* as an antiviral agent.[5−7] The compound was later identified in *Aspergillus terreus*, the producer of lovastatin.[8] Subsequent bioactivity studies have shown that **1** and its derivatives display an array of interesting biological activities, including inhibition of viral RNA polymerase,[6] induction of apoptosis in cancer cell lines,[9] and antifungal activity.[10]

The cytotoxicity of ETPs has made them therapeutically important as potential anticancer agents.[11] With the dramatic increase of fungal genome sequence information, it is now possible to identify the specific genes that are responsible for ETP production. For instance, the gene clusters that are responsible for the biosynthesis of sirodesmin PL (Figure 1) in *Leptosphaeria maculans* (*sir* cluster) and gliotoxin (Figure 1) in *A. fumigatus* (*gli* cluster) have been identified and analyzed

Received: December 18, 2012
Published: April 15, 2013

dx.doi.org/10.1021/ja3123653 | J. Am. Chem. Soc. 2013, 135, 7205−7213

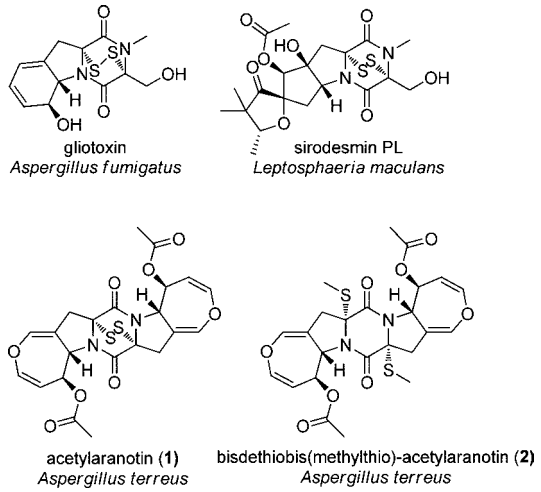

Figure 1. ETPs and their derivatives identified from different fungal species.

using bioinformatics.[12,13] Disruption of the key nonribosomal peptide synthetase (NRPS) genes *sirP* and *gliP* confirmed their involvement in the biosynthesis of the two secondary metabolites.[12,14] The function of *gliP* was further elucidated by overexpressing the gene in *Escherichia coli*. GliP is a 236 kDa three-module (A_1-T_1-C_1-A_2-T_2-C_2-T_3) NRPS. The study revealed that A_1 of GliP activates L-Phe and loads it onto T_1 while A_2 activates L-Ser and tethers it to T_2. The intramolecular cyclization is presumably catalyzed by C_1 to yield the DKP scaffold *cyclo*-L-Phe-L-Ser.[15] Previous studies have focused on the transannular disulfide bridge, which is the main contributor to gliotoxin's deleterious effects. At least five genes, *gliC*, *gliG*, *gliJ*, *gliI*, and *gliT*, are essential for the formation of this chemical moiety. GliC is believed to be a P450 monoxygenase that hydroxylates the DKP scaffold, which is followed by sulfurization by the glutathione S-transferase GliG. In the next step, the putative dipeptidase GliJ removes the Glu residues and GliI acts as a C−S lyase to yield the epidithiol moiety, which is oxidized to the disulfide bridge by the sulfhydryl oxidase GliT.[16−20]

Far less was known about the biosynthesis of acetylaranotin (Figure 1) in comparison with gliotoxin prior to this study. Acetylaranotin is characterized by the presence of two seven-membered dihydrooxepine rings. Total syntheses of **1** were recently accomplished by the Reisman group[21] and the Tokuyama group.[22] However, several obstacles have hindered an elaborate study of the biosynthesis of **1** and the potential genes involved. First, the production yield of **1** in *A. terreus* is low.[8,23−25] Second, although two candidate biosynthetic clusters for ETPs in *A. terreus* were predicted using bioinformatic analysis,[26] the lack of an efficient gene-targeting system of this fungal species has made it difficult to determine the biosynthetic pathway of **1**.

Herein we report our efforts to identify and isolate acetylaranotin and its related natural products (**2**−**5** and **16**) from wild-type *A. terreus* NIH 2624 (Figures 1 and 2). One important step in the identification of **1** and related metabolites was examining a variety of culture conditions in an effort to produce the compounds in relatively high yields. We developed a gene-deletion procedure in *A. terreus* strain NIH 2624. Targeted mutagenesis combined with metabolite analysis allowed us to identify and characterize a gene cluster containing

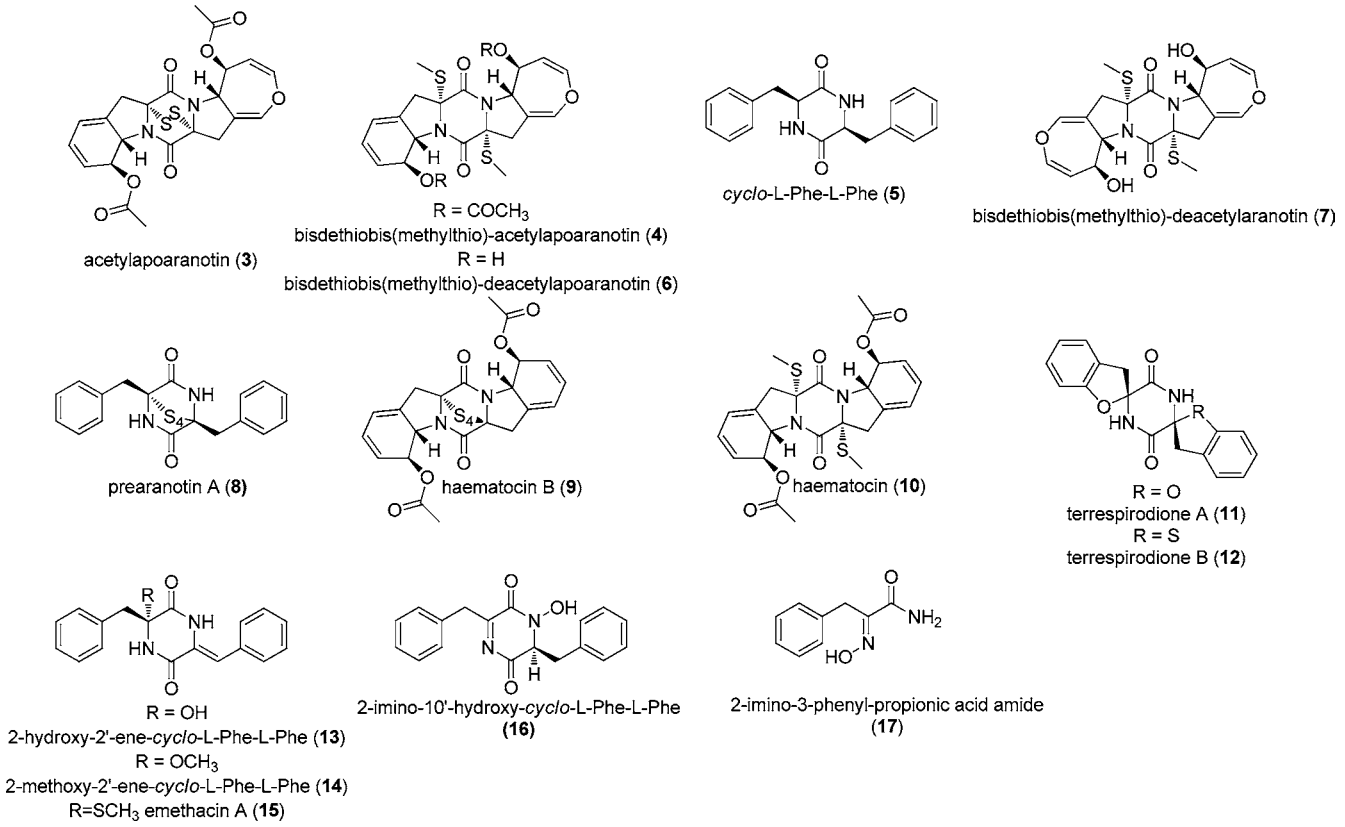

Figure 2. Natural products from the acetylaranotin biosynthesis pathway isolated in this study.

dx.doi.org/10.1021/ja3123653 | J. Am. Chem. Soc. 2013, 135, 7205−7213

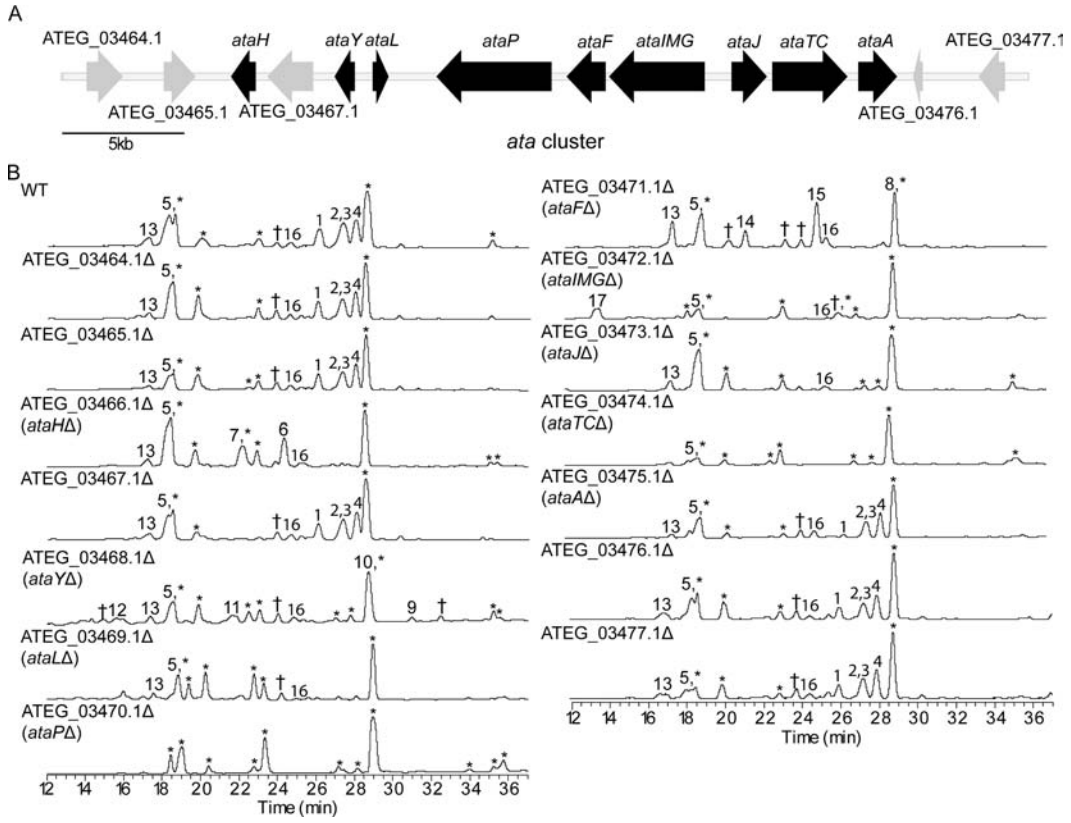

Figure 3. (A) Organization of the acetylaranotin biosynthesis gene cluster in *A. terreus*. Each arrow indicates the relative size and the direction of transcription of the open reading frames deduced from analysis of nucleotide sequences. Genes in black are involved in the biosynthesis of **1**, while those in gray are not. (B) HPLC profiles of extracts of strains in the cluster as detected by UV at total scan. The numbering of the peaks corresponds to the natural products shown in Figure 2. Peaks labeled with * correspond to compounds that can be identified in ATEG_03470.1Δ and are not involved in **1** biosynthesis. Peaks labeled with † denote compounds that could not be characterized because of poor yield or instability.

nine contiguous genes that code for the biosynthetic components responsible for the production of **1**. Targeted deletions of each of the individual genes in the cluster generated several mutants that accumulated chemically stable intermediates or shunt products in sufficient amounts for characterization. Large-scale culture of the wild-type and mutant strains enabled us to isolate a total of 17 related compounds. Nine of the identified compounds have not been reported previously. Subsequent bioinformatic analysis enabled us to propose a biosynthetic pathway for this ETP and the function of the enzymes involved in acetylaranotin biosynthesis.

RESULTS

Isolation and Characterization of 1 and Biosynthetically Related Metabolites from *A. terreus* NIH 2624. *Aspergillus* species are known to produce different secondary metabolites when cultivated under different culture conditions. By screening different culture media, we found that **1** and its related secondary metabolites (Figure 2) were produced in quantifiable yields from Czapek's medium (Figure 3). The crude organic extract of *A. terreus* growing under acetylaranotin-producing conditions was analyzed by reverse-phase liquid chromatography−diode-array detection−mass spectrometry (LC−DAD−MS), and we identified several UV peaks that were possibly related to **1** (Figure 3). For further verification, the strain was subjected to large-scale cultivation, and each peak was initially purified by flash chromatography and subsequently by preparative HPLC. Using NMR spectroscopy, we determined the structures of five known compounds, including **1**,[21] bisdethiobis(methylthio)acetylaranotin (**2**),[27] acetylapoaranotin (**3**),[7] bisdethiobis(methylthio)acetylapoaranotin (**4**),[27] and *cyclo*-L-Phe-L-Phe (**5**),[28] along with a previously unreported natural product, **16** [Figures 2 and 3; spectral data are available in the Supporting Information (SI)]. We also identified several *A. terreus* secondary metabolites that are not from the acetylaranotin pathway. Several of these compounds have been characterized and reported previously (Figure S2 in the SI).[29] The other unidentified metabolites possess chromophores different from that of **1** (Figures S1 and S2 in the SI).

Identification of the Gene Cluster Responsible for Acetylaranotin Biosynthesis. Previous bioinformatic analysis uncovered two putative ETP biosynthetic gene clusters in *A. terreus* NIH 2624.[26] Each of the two clusters contains an NRPS gene (ATEG_03470.1 in one cluster and ATEG_08427.1 in the other), one of which was likely to be responsible for the biosynthesis of the DKP scaffold of **1**. A previous study using isotopic precursors showed that compound **5** could be incorporated into compound **2**.[30] Domain analysis by searching the NCBI Conserved Domain Database (CDD) revealed that the putative protein coded by ATEG_03470.1 contains one adenylation (A) domain, whereas two such domains were identified in the amino acid sequence of ATEG_08427.1. The A domain recognizes and activates a specific amino acid or aryl acid substrate.[31] We hypothesized that ATEG_03470.1 is the NRPS gene responsible for acetylaranotin biosynthesis on the basis of the observation that only one amino acid substrate, L-Phe, is activated and condensed to form **5**. To confirm our hypothesis, we deleted

dx.doi.org/10.1021/ja3123653 | J. Am. Chem. Soc. 2013, 135, 7205−7213

Table 1. Putative Functions and Homologues of the Genes in the *ata* Cluster

gene	size (gene/aa)	characterized homologue	identity/similarity (%)	putative function
ATEG_03466.1 (*ataH*)	979/303	Tri7, *Gibberella zeae*[37]	38/57	acetyltransferase
ATEG_03468.1 (*ataY*)	795/228	MCYG_07058,[a] *Arthroderma otae* CBS 113480	33/51	benzoate *p*-hydroxylase
ATEG_03469.1 (*ataL*)	629/155	GliH, *A. fumigatus* Af293[16]	36/52	putative protein
ATEG_03470.1 (*ataP*)	4724/1507	GliP, *A. fumigatus* Af293[14,15]	30/48	NRPS
ATEG_03471.1 (*ataF*)	1572/489	GliF,[a] *A. fumigatus* Af293	50/70	epoxidase
ATEG_03472.1 (*ataIMG*)	3923/874	GliI, *A. fumigatus* Af293[20]	27/44	carbon−sulfur lyase
		GliM,[a] *A. fumigatus* Af293	41/57	*O*-methyltransferase
		GliG, *A. fumigatus* A1163[18,19]	39/56	glutathione S-transferase
ATEG_03473.1 (*ataJ*)	1437/410	GliJ,[a] *A. fumigatus* Af293	51/66	membrane dipeptidase
ATEG_03474.1 (*ataTC*)	2505/718	GliT, *A. fumigatus* Af293[16,17]	35/48	sulfhydryl oxidase
		GliC,[a] *A. fumigatus* Af293	40/59	hydroxylase
ATEG_03475.1 (*ataA*)	1581/449	GliA,[a] *A. fumigatus* Af293	35/52	MFS

[a]The functions of these enzymes have been proposed but need further verification.

the ATEG_03470.1 gene in an *A. terreus* NIH 2624 strain with a *kusA*−, *pyrG*− background and cultivated the ATEG_03470.1Δ strain under the acetylaranotin-producing conditions. The *kusA* gene deletion improved the gene-targeting efficiency because of high homologous recombination rates.[32] Analysis of the resultant secondary metabolites using LC−DAD−MS showed the complete elimination of compounds **1**−**5** and **16** (Figure 3). Thus, we confirmed the involvement of the NRPS gene ATEG_03470.1 in production of **1** and designated it as *ataP*, using the letter designation developed for ETP biosynthesis genes.[26] Metabolites that are not related to acetylaranotin biosynthesis were unaffected by the deletion of *ataP* (Figure 3).

Previous bioinformatic prediction of the putative acetylaranotin cluster suggested that several genes downstream of *ataP* encode proteins that are homologous to the enzymes involved in gliotoxin biosynthesis. These enzymes include a cytochrome P450 monooxygenase (AtaF), glutathione S-transferase (AtaG), *O*-methyltransferase (AtaM), aminocyclopropane carboxylic acid synthase (ACCS) (AtaI), dipeptidase (AtaJ), thioredoxin reductase (AtaT), cytochrome P450 monooxygenase (AtaC), and major facilitator superfamily (MFS) transporter (AtaA).[26] We chose to name the genes involved in the biosynthesis of **1** using the same letter code as developed for ETP biosynthesis (Figure 3A and Table 1).[26]

However, in the updated *Aspergillus* Comparative Database, the *A. terreus* gene ATEG_03472.1 (*ataIMG*) is annotated as a trimodular gene whose modules are homologous to gliI, gliM, and gliG (Table 1). The gene ATEG_03474.1 (*ataTC*) is annotated as a bimodular gene with homology to gliT and gliC (Table 1). We investigated the messenger RNA (mRNA) sequences of the products of these two genes using a reverse-transcription polymerase chain reaction (RT-PCR) approach. Using the complementary DNA (cDNA) of *ataIMG* as the template and the genomic DNA as the control, we were able to amplify two PCR fragments that flanked the sites where introns 1 and 8 were located in the region encoding the AtaI and AtaG domains (Figure S4 in the SI). This suggests that the mRNA of *ataIMG* includes the sequence that codes for putative AtaI and AtaG domains. Another PCR fragment flanking the site where introns 4 and 5 were located was amplified. The gene sequence spanning introns 4 and 5 includes part of the coding sequence for both the putative AtaI and AtaM domains (Figure S4). A similar strategy was applied to analyze the mRNA sequence of *ataTC*. However, one PCR fragment that flanked intron T was amplified using the cDNA of *ataTC* as the template. Intron T was not in the predicted sequence of *ataTC* but instead was found in the sequence of a putative transcript 3857_t (Figure S4A). The 3′ end of 3857_t overlaps with the 5′ end of *ataTC* by 579 base pairs. The predicted amino acid sequence of 3857_t is 48% similar to that of GliT (Table 1). The conserved motif (145-CXXC-148) in GliT, a hallmark for various sulfhydryl oxidases, was also identified in the amino acid sequence of 3857_t (145-CXXC-148) but not in that of the annotated *ataTC*.[17,33] This indicates that the coding sequence of *ataTC* is likely to cover the sequence of one putative transcript 3857_t (Figure S4; see the SI for detailed information on the transcript).

In addition, the two acetyl groups in the structure of **1** suggest the involvement of an acetyltransferase gene. Analysis of the amino acid sequences of the genes in proximity to *ataP* using the Basic Local Alignment Search Tool (BLAST) disclosed one gene, ATEG_03466.1, which we named *ataH*, that encodes a putative acetyltransferase (Table 1). We then suspected that the three genes between *ataH* and *ataP* could also be involved. In all, an additional nine genes from *ataH* to *ataA* flanking the NRPS gene *ataP* were selected for deletion experiments. Four additional genes flanking the cluster, ATEG_03464.1, ATEG_03465.1, ATEG_03476.1, and ATEG_03477.1, were also selected for deletion analysis. Our bioinformatic analysis suggested that these four genes are beyond the acetylaranotin biosynthetic gene cluster and that examination of their secondary metabolite profiles would enable us to determine the two boundaries of the cluster.

The genes were individually deleted following the previously developed protocol.[29] Two verified deletants of each gene were cultivated under acetylaranotin-producing conditions. Examination of the LC−MS profiles of the mutant strains revealed that ATEG_03466.1Δ (*ataH*Δ), ATEG_03468.1Δ (*ataY*Δ), ATEG_03469.1Δ (*ataL*Δ), ATEG_03470.1Δ (*ataP*Δ), ATEG_03471.1Δ (*ataF*Δ), ATEG_03472.1Δ (*ataIMG*Δ), ATEG_03473.1Δ (*ataJ*Δ), ATEG_03474.1Δ (*ataTC*Δ), and ATEG_03475.1Δ (*ataA*Δ) impaired the production of compounds **1**−**4** (Figure 3), indicating that these nine genes are involved in the biosynthesis of **1**. The ATEG_03467.1Δ strain continued to produce **1** and its related natural products, suggesting that this gene, which codes for a putative MFS transporter, is not involved in the biosynthesis pathway (Figure 3). As predicted, the secondary metabolite profiles remained unchanged after deletion of the genes ATEG_03464.1, ATEG_03465.1, ATEG_03476.1, and ATEG_03477.1, indicating that these four genes are not involved in the biosynthesis of

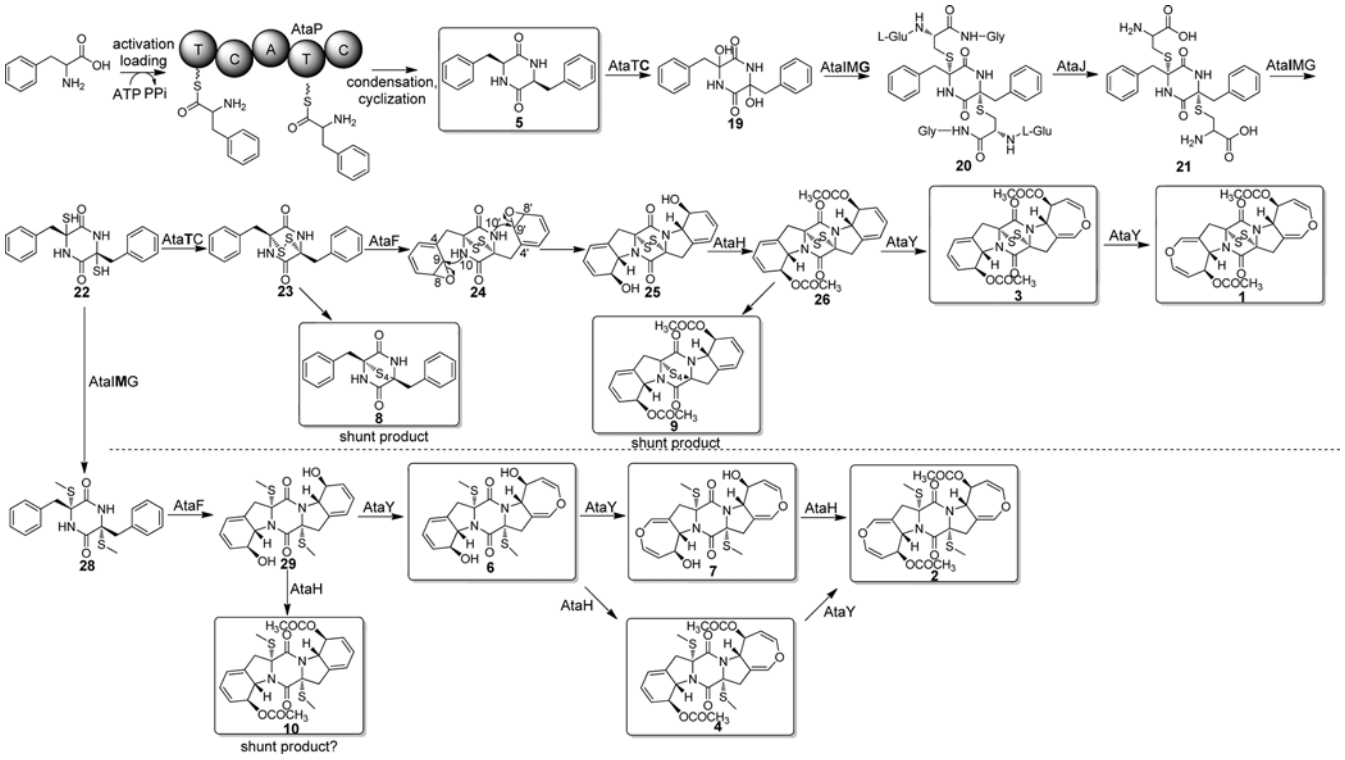

Figure 4. Proposed biosynthetic pathway for **1** and its methylated form **2**. The pathway bifurcates to **1** and **2** and is separated by a dashed line at this point. For proteins with fused catalytic domains, the domain that is active at a particular step is shown in bold. All of the natural products isolated in this study are boxed.

1 and that we have defined the two boundaries of the cluster (Figure 3).

Identification, Purification, and Structural Determination of the Intermediates and Shunt Products from Mutant Strains. Compound **5** was still identified in the metabolite profiles of all of the deletion strains except the *ataP*Δ strain, suggesting that **5** may be the first intermediate synthesized by AtaP (Figure 3). However, we cannot exclude the alternative that **5** stands as a shunt product that could be derived from the nonenzymatic cyclization of tethered dityrosine.

Mutant strains containing gene replacements of four genes, *ataH*, *ataY*, *ataF*, and *ataIMG*, accumulated amounts of chemically stable intermediates or shunt products that were sufficient for structure determination (Figure 3). The two natural products **6** and **7** were purified from scaled-up cultures of the *ataH*Δ strain (Figures 2 and 3). Compound **6** was previously isolated from *Menisporopsis theobromae*.[34] We confirmed the structure of **7** using one-dimensional (1D) and two-dimensional (2D) NMR spectroscopy (see the SI for detailed information). Both compounds have carbon skeletons similar to that of **1**, suggesting that the acetylation of **1** occurs in the later stage of its biosynthesis. From the culture of the *ataY*Δ strain, we purified and characterized the four secondary metabolites **9**–**12** (Figures 2 and 3). Compound **10** was previously reported as haematocin, an antifungal DKP isolated from *Nectria hematococca*, a fungus causing nectria blight disease on ornamental plants.[10] Compounds **9**, **11**, and **12** are previously unreported compounds, and their structures were elucidated via a complete 1D and 2D NMR and high-resolution electrospray ionization MS analysis (see the SI for detailed information). The epitetrasulfide bridge found in **9** is also present in gliotoxin G, which is a derivative of the disulfide gliotoxin.[35] Compounds **8**, **13**, **14**, and **15** isolated from large-scale cultures of the *ataF*Δ strain all are derivatives of the dipeptide compound **5** (Figures 2 and 3). Reexamination of the LC–MS profiles revealed that **13** was also produced in the wild type and the other mutant strains, except for the *ataP*Δ, *ataIMG*Δ, and *ataTC*Δ strains (Figure 3). Removal of the *ataF* gene led to the accumulation of this minor metabolite, making its analysis by NMR spectroscopy feasible. We were also able to purify and resolve the structure of **17** from the *ataIMG*Δ strain (Figures 2 and 3). Surprisingly, metabolite **17** no longer maintains the DKP scaffold, indicating that it might be a shunt product involved in acetylaranotin biosynthesis.

For better differentiation between the intermediates and shunt products isolated in our study, compounds **4**–**7** and **10** were fed into the *ataP*Δ strain under acetylaranotin-producing conditions. We hypothesized that if one compound is an intermediate, feeding it into the *ataP*Δ strain might recover some of the strain's ability to reproduce its downstream natural products in the pathway. We detected the accumulation of compound **2** in the extract of the *ataP*Δ strain after feeding with compound **4** (Figure S6A in the SI). Compounds **1**, **2**, and **4** were detected after feeding with compound **5** (Figure S6B). We identified compound **4** after feeding with substrate **6** (Figure S6C) and compound **2** after feeding substrate **7** (Figure S6D). Our data suggest that compounds **4**–**7** are likely the intermediates involved in the biosynthesis of **1** or its methylated form **2** (Figures 4 and S6). No downstream metabolites were identified after feeding with compound **10** (Figure S6E), indicating that it is likely a shunt product in the biosynthesis of **2** or alternatively that it might not be able to cross the cell wall (Figure 4).

dx.doi.org/10.1021/ja3123653 | J. Am. Chem. Soc. 2013, 135, 7205–7213

DISCUSSION

We used a combination of genomics, efficient gene targeting, and natural product chemistry to identify the genes encoding the biosynthesis pathway for the ETP toxin acetylaranotin (**1**) in *A. terreus*. After optimal culture conditions for the production of **1** were found, we embarked on a targeted gene knockout approach to identify the genes involved in the biosynthesis pathway. We showed that the acetylaranotin biosynthesis pathway is complex and involves the products of at least nine clustered genes. In addition to **1**, 16 additional compounds produced from the pathway were isolated. Nine of these compounds have not been reported previously. Bioinformatic analysis of the responsible genes, along with comparison to the similar gliotoxin biosynthesis pathway, has allowed us to propose a biosynthetic pathway for **1**.

In our proposed pathway, the first gene, *ataP*, encodes an NRPS for the biosynthesis of diketopiperazine **5**. AtaP has the domain architecture (T_1-C_1-A_1-T_2-C_2). AtaP shares 48% similarity to GliP, the NRPS in the gliotoxin pathway (Table 1).[14,15] The single A domain in AtaP suggests that one specific substrate, L-Phe, is loaded onto the T domains of AtaP. The sequence of the AtaP A domain was aligned with several A domains of fungal NRPSs that have been shown to accept phenylalanine as their substrate (Figure S7 in the SI). The alignment showed several conserved motifs that might be involved in phenylalanine selection and activation by these A domains, but further investigation is necessary to define the A-domain signature motifs for amino acid recognition in fungal NRPSs. A previous study using isotopic precursors showed the intact incorporation of compound **5** into compound **2** in *A. terreus*.[30] We were able to detect the accumulation of **5** in all of the mutant strains except the *ataP*Δ strain (Figure 3), indicating that **5** is an early precursor involved in the biosynthesis of **1**.

Five genes (*gliC*, *gliG*, *gliJ*, *gliI*, and *gliT*) are proposed to be involved in the sulfurization of the *cyclo*-L-Phe-L-Ser DKP skeleton in gliotoxin biosynthesis.[16−20] In addition, a sixth gene encoding the *O*-methyltransferase GliM may catalyze the methylation of the free thiols.[18,36] Homologues of these six gliotoxin genes can be identified in the acetylaranotin gene cluster in *A. terreus* (Table 1). We propose that the AtaC domain of AtaTC catalyzes the bishydroxylation of compound **5** to yield intermediate **19** (Figure 4). The *ataTC*Δ strain failed to produce any detectable intermediates or shunt products from the pathway except **5**, providing evidence that the dual hydroxylation is an early step in the biosynthesis pathway (Figures 3 and 4). The glutathione S-transferase domain AtaG in AtaIMG catalyzes the conjugation of two glutathiones to bishydroxylated **19** to give precursor **20**, similar to the role of GliG in gliotoxin biosynthesis (Figure 4).[18,19] Next, we propose that the dipeptidase AtaJ removes the Glu residues of intermediate **20** to give **21** on the basis of the proposed function of its homologue GliJ (Figure 4 and Table 1).[18] From the *ataJ*Δ strain, we were able to identify intermediate **5** and two shunt metabolites **13** and **16**. These compounds do not contain a pyrrolidine ring moiety as shown in **1**, suggesting that AtaJ is involved in the early steps of acetylaranotin biosynthesis. Next, the carbon−sulfur lyase domain AtaI of AtaIMG may catalyze a similar reaction to GliI, converting biscysteinyl adduct **21** to epidithiol intermediate **22** (Figure 4). The purification of shunt product **8** projected the existence of intermediate **23** (Figure 4). On the basis of homology and the conserved CXXC motif, we propose that the AtaT domain identified in the adjusted AtaTC protein sequence catalyzes the oxidation of the free dithiols in precursor **22** to yield **23**.

Next, the cyclization of **23** to give intermediate **25** may be catalyzed by the cytochrome P450 AtaF. From the *ataF*Δ strain, we identified compounds **5**, **8**, and **13**−**16** (Figure 3). The pyrrolidine structure in **1** is noticeably missing in these compounds (Figure 2). AtaF shares 70% similarity to GliF, which has not been characterized genetically or biochemically. AtaF probably acts as an epoxidase to promote dual epoxidation at C8 and C9 along with C8′ and C9′ of **24**, which is followed by the spontaneous nucleophilic attack of the amide nitrogens N10 and N10′ of **24** to yield **25** with the pyrrolidine partial structure (Figure 4).

The final steps of acetylaranotin biosynthesis involve the acetylation and ring rearrangement of intermediate **25** to produce **1**. These transformations are not found in the gliotoxin biosynthesis pathway. Therefore, the genes involved in the transformation from **25** to **1** may not have homologues in the gliotoxin gene cluster. AtaH has 57% amino acid similarity to Tri7 of *Gibberella zeae* (Table 1). Tri7 has been shown to be involved in the acetylation of the oxygen at C4 of nivalenol.[37] AtaY has 51% similarity with a putative benzoate *p*-hydroxylase found in *Arthroderma otae* CBS 113480. The benzoate *p*-hydroxylase homologue (CYP51A) in *Aspergillus niger* was purified and characterized previously.[38] We propose that AtaH catalyzes the acetylation of **25** to **26** and that AtaY is responsible for the formation of the dihydrooxepin moiety that converts **26** to **1** via compound **3** (Figure 4 and Table 1). Our data suggest that each of these enzymes can function independently in the absence of the other. From the *ataH*Δ strain, we were able to isolate putative intermediates **6** and **7**, which are not acetylated but contain the dihydrooxepine partial structure. From the *ataY*Δ strain, we were able to identify compounds **5**, **9**−**13**, and **16**. None of these compounds have the dihydrooxepine partial structure. The isolation of tetrasulfide **9** projected the existence of intermediate **26** in the biosynthesis of **1**. The acetyl groups of **9** suggest that the acetylation step can still occur in the absence of AtaY.

We identified an MFS transporter, AtaA, encoded in the acetylaranotin biosynthesis cluster. The MFS genes found in secondary metabolite gene clusters sometimes code for transporters that are involved in the specific efflux of a secondary metabolite. Tri12, for instance, plays a role in the transport of trichothecene in *Fusarium* species.[39] In the *ataA*Δ strain, we observed that the production of **1** was greatly reduced. This suggests that AtaA could be involved in the efflux of **1** or that the *ataA* deletion could lead to a degradation product of **1** that cannot be secreted. It is also possible that *ataA* deletion could downregulate the biosynthesis of **1**, but it should be noted that other compounds (**2**−**5**, **13**, and **16**) are produced in the *ataA*Δ strain at levels comparable to those in the wild-type strain (Figure 3). Thus, the function of AtaA is still not clear and awaits further investigation.

There is another gene, ATEG_03469.1 (*ataL*), for which we were not able to definitively assign the function of its putative product. BLAST analysis of AtaL revealed that it has an uncharacterized ligand-binding domain and is 52% similar to GliH (Table 1). A previous study reported that deletion of *gliH* abolished gliotoxin production, suggesting that this gene is involved in gliotoxin biosynthesis or secretion.[16] Only compounds **5**, **13**, and **16** could be identified in the secondary metabolite profiles of the *ataL*Δ strain, indicating that it may be

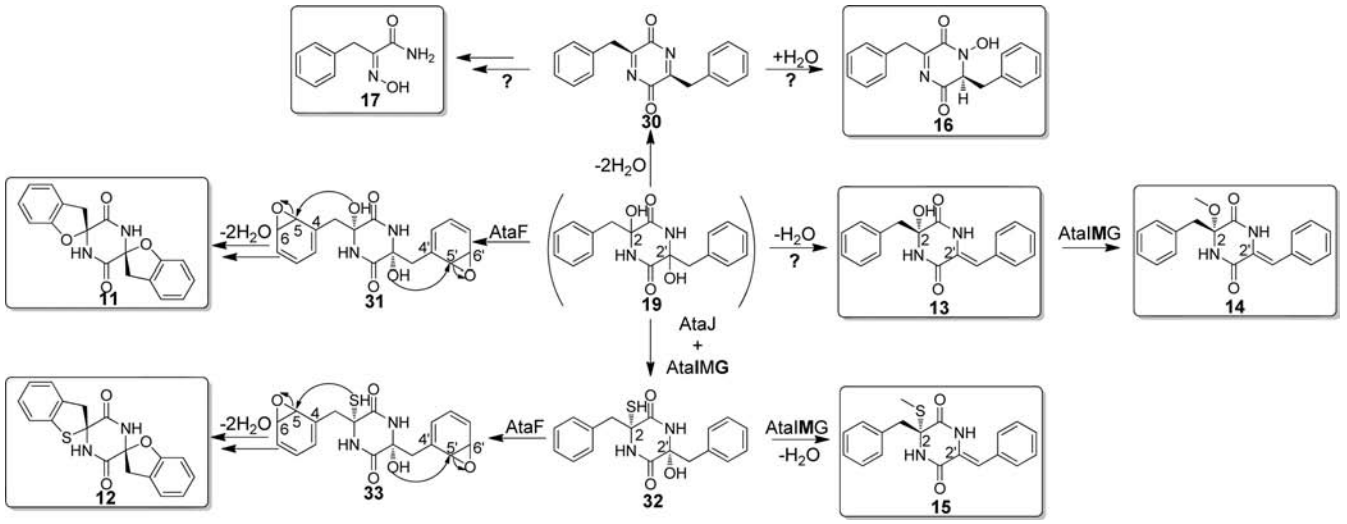

Figure 5. Additional shunt pathways in acetylaranotin biosynthesis. For proteins with fused catalytic domains, the domain that is active at a particular step is shown in bold. The starting molecule **19** is shown in parentheses. All of the compounds isolated in this study are boxed.

involved in the conversion of the C−O bond in **19** to the C−S bond in **22** or in the secretion of **1** and its related natural products. However, additional experiments will be necessary to clarify further the specific function of AtaL.

Methylation of the free dithiols of precursor **22** seems to be a branching point for the biosynthesis of **1** and its sulfur-methylated form **2** (Figure 4). We propose that the AtaM domain of AtaIMG, a homologue of the putative *S*-methyltransferase GliM (Table 1), is responsible for this methylation step. Methylation of **22** by the AtaM domain of AtaIMG gives **28**, and subsequent AtaF-catalyzed cyclization converts **28** to **29**. Ring expansion by AtaY converts **29** to **7** via intermediate **6**, and acetylation by AtaH produces compound **2**. Another pathway that converts **6** to **2** involves acetylation of **6** by AtaH to produce intermediate **4** followed by ring expansion by AtaY that converts **4** to **2**.

Other shunt products in acetylaranotin biosynthesis (**11**−**17**) were also isolated from the gene-deletion strains (Figure 5). Two molecules of water are probably eliminated from **19** to yield an unstable imine **30**, N-hydroxylation of which produces **16** (Figure 5). Compound **17**, isolated from the *ataIMG*Δ strain, no longer maintains the DKP framework, suggesting that other genes beyond the *ata* cluster could be involved in its formation. The 2′ olefinic moiety found in **13**−**15** is probably formed via the elimination of one water molecule at C2′ of **19** (Figure 5). Methylation of the C2 hydroxyl group in **14** and the C2 thiol in **15** could be catalyzed by the AtaM domain of AtaIMG.

We were able to isolate two shunt products, **11** and **12**, from the *ataY*Δ strain. We hypothesized that AtaF is capable of catalyzing dual epoxidation at C5 and C6 along with C5′ and C6′ of **19** to produce intermediate **31**, with subsequent spontaneous nucleophilic attack initiated by the free hydroxyl groups at C2 and C2′ leading to the formation of the spiro partial structure in **11** (Figure 5). This mechanism was mentioned in a previous study to explain the formation of two gliotoxin shunt products with a spiro partial structure.[36] The formation of compound **12** seems more complex. Sulfurization at C2 of intermediate **19**, yielding C2 thiol intermediate **32**, likely involves AtaJ and AtaIMG. AtaF then catalyzes the epoxidation of **32** to **33**, which spontaneously converts to **12** (Figure 5). The formation of the spiro shunt products **11** and **12** is probably due to substitution of the corresponding benzene oxide intermediates **31** and **33** by the more nucleophilic hydroxyl or thiol groups. Formation of the epidisulfide bridge or methylation of the free thiols or hydroxyls might reduce their nucleophilicity and enable oxide intermediate **24** to be attacked by the amide nitrogen to give the pyrrolidine partial structure shown in **1**.

Previous studies proposed that the reduced oxepine moiety shown in compounds **1**−**4** is formed via equilibrium with its arene oxide tautomeric components prior to the pyrrolidine ring cyclization.[6,7] The epoxidation of the oxepine ring then generates a *sym*-oxepine oxide moiety that is attacked by the nucleophilic amide nitrogen to give the pyrrolidine moiety.[6,7] Indeed, it is known that benzene oxide and oxepine exist in valence-tautomeric equilibrium with each other.[40] Though the calculated energy of benzene oxide is 1.7 kcal mol^{-1} lower than that of oxepine, the equilibrium favors the oxepine form at room temperature because of the associated entropy gain ($\Delta G \approx -1.3$ kcal mol^{-1}).[40] The epoxide intermediates **24** (involved in pyrrolidine ring cyclization), **31**, and **33** (involved in spiro shunt product biosynthesis) are therefore likely to be in equilibrium with their more favorable oxepine forms (Figures 4 and 5). However, the methylene substitution at the 4 and 4′ positions of these intermediates (Figures 4 and 5) may shift the equilibrium toward their oxide forms, which may undergo nucleophilic substitution.[40,41] In our study, we identified compound **2** in the total extract of the *ataP*Δ strain after feeding the strain with compound **4** under acetylaranotin-producing conditions (Figure 4 and Figure S6A in the SI). This suggests that formation of the oxepine moiety could occur after cyclization of the pyrrolidine ring. Further investigation focusing on the catalytic function of AtaY will help to elucidate the mechanism involved in the formation of the dihydrooxepine rings in **1**.

Another interesting aspect is the self-protection strategy adapted by *A. terreus* against the toxin **1**. GliT mediates self-resistance of *A. fumigatus* against gliotoxin. Removal of *gliT* accumulates the metabolite with free dithiols, which may generate ROS or protein conjugates.[16,17] We did not observe any growth inhibition of wild-type *A. terreus* under acetylaranotin-producing conditions, suggesting that the AtaT domain functions normally. A recent study suggested that S-

dx.doi.org/10.1021/ja3123653 | J. Am. Chem. Soc. 2013, 135, 7205−7213

methylation of holomycin intermediates serves as another self-protection strategy taken by *Streptomyces clavuligerus*.[42] Compounds **1** and **3** with an epidisulfide bridge and the corresponding S-methylated forms **2** and **4** were identified, suggesting that *A. terreus* deploys both autoprotection strategies. The methylated sulfhydryl groups are less readily converted to dithiols compared with the disulfide moiety. Therefore, the cellular toxicity of the methylated forms may be reduced.[42]

CONCLUSION

Using a targeted gene-deletion approach, we have shown that a total of nine clustered genes are involved in the biosynthesis of the ETP toxin acetylaranotin (**1**) in *A. terreus*. By combining bioinformatic data and intermediates or shunt products isolated from the individual gene deletion mutants, we have proposed a biosynthetic pathway for **1**.

MATERIALS AND METHODS

Strains and Molecular Manipulations. The primers used in this study are listed in Table S1 in the SI, and the *A. terreus* wild-type and mutant strains used in this project are listed in Table S2 in the SI. Each targeted gene was individually deleted by the *A. fumigatus pyrG* gene (*AfpyrG*) in the *kusA*−, *pyrG*− background of *A. terreus*. The construction of double joint-fusion PCR products, protoplast generation, and transformation were carried out according to previously published procedures.[29] Three putative gene replacements for each gene were randomly picked and verified by diagnostic PCR. At least two of the three transformants were determined to be correct for each gene (see the SI for more information). The scheme of diagnostic PCR of the mutant strains is presented in Figure S3 in the SI. The difference in size between the gene replaced by the resistant marker and the native gene allowed us to determine whether the transformants carried the correct gene replacement. When the targeted gene size was similar to the marker *AfpyrG*, an internal primer that specifically binds to *AfpyrG* was used with an outside primer. When the targeted gene was successfully replaced by *AfpyrG*, a PCR fragment of around 4 kb could be amplified from the mutant strains (Figure S5 in the SI).

RT-PCR Analyses. The *A. terreus* wild-type strain was cultivated under acetylaranotin-producing conditions for 72 h. Total RNA of the *A. terreus* wild-type strain was extracted using the Qiagen RNeasy Plant Mini Kit according to the manufacturer's instructions. Contaminating DNA was removed by digestion with DNase I (Fermentas). The cDNA was synthesized with the specific primers ATEG_03472.1RT and ATEG_03474.1RT (Table S1 in the SI) using TaqMan Reverse Transcription Reagents (Applied Biosystems) following the supplied protocols. The cDNA was then used as the template for PCR amplification with specific primer sets of ATEG_03472.1 and ATEG_03474.1 flanking the putative introns (Figure S4 and Table S1 in the SI). Amplification products were analyzed by electrophoresis in 1% agarose gels stained with ethidium bromide.

Fermentation and LC−MS Analysis. The wild-type and mutant *A. terreus* strains were cultivated at 30 °C on Czapek's agar plates ($NaNO_3$, 3 g/L; KCl, 0.5 g/L; $MgSO_4{\cdot}7H_2O$, 0.50 g/L; K_2HPO_4, 1.0 g/L; $FeSO_4{\cdot}7H_2O$, 0.01 g/L; sucrose, 30 g/L; agar, 15 g/L) at 20×10^6 spores per 10 cm plate. After 5 days, the agar was chopped into small pieces and extracted with 50 mL of 1:1 CH_2Cl_2/MeOH with sonication for 1.0 h. The extract was evaporated in vacuo to yield a water residue, which was suspended in 25 mL of water and partitioned with 25 mL of ethyl acetate (EA). The EA layer was evaporated in vacuo and redissolved in 1 mL of 20% dimethyl sulfoxide/MeOH, and a 10 μL portion was examined by HPLC−DAD−MS analysis. HPLC−MS was carried out using a Thermo Finnigan LCQ Advantage ion trap mass spectrometer with a reverse-phase C18 column (Alltech Prevail C18 2.1 mm × 100 mm with a 3 μm particle size) at a flow rate of 125 μL/min. The solvent gradient system for HPLC and the conditions for MS analysis were described previously.[29]

Isolation and Characterization of Secondary Metabolites. For structure elucidation, the *A. terreus* wild-type and mutant strains were cultivated on forty Czapek's agar plates (~50 mL of medium per plate, D = 15 cm) at 30 °C for 5 days. The UV-active secondary metabolites were isolated via flash chromatography and reverse-phase HPLC. A 10 μL portion of each purified compound solution from the reverse-phase HPLC was then examined using an Agilent Technologies 1200 series high-resolution mass spectrometer. Melting points were measured with a Yanagimoto micromelting point apparatus and were uncorrected. IR spectra were recorded on a GlobalWorks Cary 14 spectrophotometer. Optical rotations were measured on a JASCO P-200 digital polarimeter. NMR spectra were collected on a Varian Mercury Plus 400 spectrometer (see the SI for more details).

ASSOCIATED CONTENT

Supporting Information

A. terreus strains and primers used in this study, detailed structure characterization, purification methods, RT-PCR and diagnostic PCR results, feeding experiment results, and NMR spectral data. This material is available free of charge via the Internet at http://pubs.acs.org.

AUTHOR INFORMATION

Corresponding Author

clayw@usc.edu

Notes

The authors declare no competing financial interest.

ACKNOWLEDGMENTS

The project described was supported in part by PO1GM084077 from the National Institute of General Medical Sciences to C.C.C.W. Research conducted at the Pacific Northwest National Laboratory was supported by the Department of Energy, Office of the Biomass Program. The research group of C.C.C.W. was additionally supported by the Snyder Foundation.

REFERENCES

(1) Gardiner, D. M.; Waring, P.; Howlett, B. J. *Microbiology* **2005**, *151*, 1021−1032.
(2) Fox, E. M.; Howlett, B. J. *Mycol. Res.* **2008**, *112*, 162−169.
(3) Pardo, J.; Urban, C.; Galvez, E. M.; Ekert, P. G.; Müller, U.; Kwon-Chung, J.; Lobigs, M.; Müllbacher, A.; Wallich, R.; Borner, C.; Simon, M. M. *J. Cell. Biol.* **2006**, *174*, 509−519.
(4) Pahl, H. L.; Krauß, B.; Schulze-Osthoff, K.; Decker, T.; Traenckner, E. B.-M.; Vogt, M.; Myers, C.; Parks, T.; Warring, P.; Mühlbacher, A.; Czernilofsky, A. P.; Baeuerle, P. A. *J. Exp. Med.* **1996**, *183*, 1829−1840.
(5) Nagarajan, R.; Huckstep, L. L.; Lively, D. H.; DeLong, D. C.; Marsh, M. M.; Neuss, N. *J. Am. Chem. Soc.* **1968**, *90*, 2980−2982.
(6) Neuss, N.; Boeck, L. D.; Brannon, D. R.; Cline, J. C.; DeLong, D. C.; Gorman, M.; Huckstep, L. L.; Lively, D. H.; Mabe, J.; Marsh, M. M.; Molloy, B. B.; Nagarajan, R.; Nelson, J. D.; Stark, W. M. *Antimicrob. Agents Chemother.* **1968**, 213−219.
(7) Neuss, N.; Nagarajan, R.; Molloy, B. B.; Huckstep, L. L. *Tetrahedron Lett.* **1968**, *9*, 4467−4471.
(8) Miller, P. A.; Trown, P. W.; Fulmor, W.; Morton, G. O.; Karliner, J. *Biochem. Biophys. Res. Commun.* **1968**, *33*, 219−221.
(9) Choi, E. J.; Park, J. S.; Kim, Y. J.; Jung, J. H.; Lee, J. K.; Kwon, H. C.; Yang, H. O. *J. Appl. Microbiol.* **2011**, *110*, 304−313.
(10) Suzuki, Y.; Takahashi, H.; Esumi, Y.; Arie, T.; Morita, T.; Koshino, H.; Uzawa, J.; Uramoto, M.; Yamaguchi, I. *J. Antibiot. (Tokyo)* **2000**, *53*, 45−49.

(11) Vigushin, D.; Mirsaidi, N.; Brooke, G.; Sun, C.; Pace, P.; Inman, L.; Moody, C.; Coombes, R. *Med. Oncol.* **2004**, *21*, 21−30.
(12) Gardiner, D. M.; Cozijnsen, A. J.; Wilson, L. M.; Pedras, M. S.; Howlett, B. *J. Mol. Microbiol.* **2004**, *53*, 1307−1318.
(13) Gardiner, D. M.; Howlett, B. J. *FEMS Microbiol. Lett.* **2005**, *248*, 241−248.
(14) Cramer, R. A., Jr.; Gamcsik, M. P.; Brooking, R. M.; Najvar, L. K.; Kirkpatrick, W. R.; Patterson, T. F.; Balibar, C. J.; Graybill, J. R.; Perfect, J. R.; Abraham, S. N.; Steinbach, W. J. *Eukaryotic Cell* **2006**, *5*, 972−980.
(15) Balibar, C. J.; Walsh, C. T. *Biochemistry* **2006**, *45*, 15029−15038.
(16) Schrettl, M.; Carberry, S.; Kavanagh, K.; Haas, H.; Jones, G. W.; O'Brien, J.; Nolan, A.; Stephens, J.; Fenelon, O.; Doyle, S. *PLoS Pathog.* **2010**, *6*, No. e1000952.
(17) Scharf, D. H.; Remme, N.; Heinekamp, T.; Hortschansky, P.; Brakhage, A. A.; Hertweck, C. *J. Am. Chem. Soc.* **2010**, *132*, 10136−10141.
(18) Davis, C.; Carberry, S.; Schrettl, M.; Singh, I.; Stephens, J. C.; Barry, S. M.; Kavanagh, K.; Challis, G. L.; Brougham, D.; Doyle, S. *Chem. Biol.* **2011**, *18*, 542−552.
(19) Scharf, D. H.; Remme, N.; Habel, A.; Chankhamjon, P.; Scherlach, K.; Heinekamp, T.; Hortschansky, P.; Brakhage, A. A.; Hertweck, C. *J. Am. Chem. Soc.* **2011**, *133*, 12322−12325.
(20) Scharf, D. H.; Chankhamjon, P.; Scherlach, K.; Heinekamp, T.; Roth, M.; Brakhage, A. A.; Hertweck, C. *Angew. Chem., Int. Ed.* **2012**, *51*, 10064−10068.
(21) Codelli, J. A.; Puchlopek, A. L.; Reisman, S. E. *J. Am. Chem. Soc.* **2012**, *134*, 1930−1933.
(22) Fujiwara, H.; Kurogi, T.; Okaya, S.; Okano, K.; Tokuyama, H. *Angew. Chem., Int. Ed.* **2012**, *51*, 13062−13065.
(23) Haritakun, R.; Rachtawee, P.; Chanthaket, R.; Boonyuen, N.; Isaka, M. *Chem. Pharm. Bull.* **2010**, *58*, 1545−1548.
(24) Kamata, S.; Sakai, H.; Hirota, A. *Agric. Biol. Chem.* **1983**, *47*, 2637−2638.
(25) Haritakun, R.; Rachtawee, P.; Komwijit, S.; Nithithanasilp, S.; Isaka, M. *Helv. Chim. Acta* **2012**, *95*, 308−313.
(26) Patron, N. J.; Waller, R. F.; Cozijnsen, A. J.; Straney, D. C.; Gardiner, D. M.; Nierman, W. C.; Howlett, B. J. *BMC Evol. Biol.* **2007**, *7*, 174.
(27) Lin, Z.; Zhu, T.; Fang, Y.; Gu, Q. *Magn. Reson. Chem.* **2008**, *46*, 1212−1216.
(28) Wang, J. M.; Ding, G. Z.; Fang, L.; Dai, J. G.; Yu, S. S.; Wang, Y. H.; Chen, X. G.; Ma, S. G.; Qu, J.; Xu, S.; Du, D. *J. Nat. Prod.* **2010**, *73*, 1240−1249.
(29) Guo, C.-J.; Knox, B. P.; Chiang, Y.-M.; Lo, H.-C.; Sanchez, J. F.; Lee, K.-H.; Oakley, B. R.; Bruno, K. S.; Wang, C. C. C. *Org. Lett.* **2012**, *14*, 5684−5687.
(30) Boente, M. I. P.; Kirby, G. W.; Robins, D. J. *J. Chem. Soc., Chem. Commun.* **1981**, 619−621.
(31) Fischbach, M. A.; Walsh, C. T. *Chem. Rev.* **2006**, *106*, 3468−3496.
(32) Ninomiya, Y.; Suzuki, K.; Ishii, C.; Inoue, H. *Proc. Natl. Acad. Sci. U.S.A.* **2004**, *101*, 12248−12253.
(33) Heckler, E. J.; Rancy, P. C.; Kodali, V. K.; Thorpe, C. *Biochim. Biophys. Acta* **2008**, *1783*, 567−577.
(34) Chinworrungsee, M.; Kittakoop, P.; Saenboonrueng, J.; Kongsaeree, P.; Thebtaranonth, Y. *J. Nat. Prod.* **2006**, *69*, 1404−1410.
(35) Kirby, G. W.; Rao, G. V.; Robins, D. J. *J. Chem. Soc., Perkin Trans. 1* **1988**, 301−304.
(36) Forseth, R. R.; Fox, E. M.; Chung, D.; Howlett, B. J.; Keller, N. P.; Schroeder, F. C. *J. Am. Chem. Soc.* **2011**, *133*, 9678−9681.
(37) Lee, T.; Han, Y.-K.; Kim, K.-H.; Yun, S.-H.; Lee, Y.-W. *Appl. Environ. Microbiol.* **2002**, *68*, 2148−2154.
(38) Faber, B. W.; van Gorcom, R. F.; Duine, J. A. *Arch. Biochem. Biophys.* **2001**, *394*, 245−254.
(39) Alexander, N. J.; McCormick, S. P.; Hohn, T. M. *Mol. Gen. Genet.* **1999**, *261*, 977−984.
(40) Vogel, E.; Günther, H. *Angew. Chem., Int. Ed. Engl.* **1967**, *6*, 385−401.
(41) Hayes, D. M.; Nelson, S. D.; Garland, W. A.; Kollman, P. A. *J. Am. Chem. Soc.* **1980**, *102*, 1255−1262.
(42) Li, B.; Forseth, R. R.; Bowers, A. A.; Schroeder, F. C.; Walsh, C. T. *ChemBioChem* **2012**, *13*, 2521−2526.